

Structure Formation due to Antagonistic Salts

Akira Onuki^{a*}, Shunsuke Yabunaka^b, Takeaki Araki^a, Ryuichi Okamoto^c

^a Department of Physics, Kyoto University, Kyoto 606-8502, Japan

^b Yukawa Institute for Theoretical Physics, Kyoto University, Kyoto 606-8502, Japan

^c Department of Chemistry, Tokyo Metropolitan University, Hachioji, Tokyo 192-0397, Japan

(Dated: April 5, 2016)

Antagonistic salts are composed of hydrophilic and hydrophobic ions. In a mixture solvent (water-oil) such ion pairs are preferentially attracted to water or oil, giving rise to a coupling between the charge density and the composition. First, they form a large electric double layer at a water-oil interface, reducing the surface tension and producing mesophases. Here, the cations and anions are loosely bound by the Coulomb attraction across the interface on the scale of the Debye screening length. Second, on solid surfaces, hydrophilic (hydrophobic) ions are trapped in a water-rich (oil-rich) adsorption layer, while those of the other species are expelled from the layer. This yields a solvation mechanism of local charge separation near a solid. In particular, near the solvent criticality, disturbances around solid surfaces can become oscillatory in space. In mesophases, we calculate periodic structures, which resemble those in experiments.

Keywords: antagonistic salt, selective solvation, mesophases, ion adsorption, charge inversion

I. INTRODUCTION

In soft materials, much attention has been paid to the Coulomb interaction among charged objects. However, not enough attention has yet been paid to the solvation (or hydration) interaction between ions and polar solvent molecules [1], particularly when ions induce some phase ordering [2]. In liquid water, small metallic ions are surrounded by several water molecules to form a hydration shell due to the ion-dipole interaction. As a result, such ions are strongly hydrophilic. On the other hand, hydrophobic ions have been used in electrochemistry [2]. An example is tetraphenylborate BPh_4^- with a diameter about 0.9 nm consisting of four phenyl rings bonded to a negatively ionized boron (see Fig.1). Because of its large size, it largely deforms the surrounding hydrogen bonding acquiring strong hydrophobicity [3].

In this review, we explain some unique effects emerging when both hydrophilic and hydrophobic ions are present in a mixture solvent composed of water and a less polar component (called oil). In this situation, such cations and anions behave *antagonistically* in the presence of composition heterogeneity and even induce mesophases with charge density waves. As in Fig.1, they tend to segregate around a water-oil interface due to the selective solvation, but they can only undergo microphase separation on the scale of the Debye screening length due to the Coulomb attraction [4]. Indeed, in a x-ray reflectivity experiment, Luo *et al.* [5] observed such ion distributions around a water-nitrobenzene interface. The resultant electric double layer reduces the surface tension γ [6–8]. Such a decrease in γ was recently observed [9]. Thus, with an antagonistic salt in the vicinity of the solvent criticality, we have $\gamma < 0$ to find mesophases.

Sadaka *et al.* [10, 11] detected a peak in the small-angle neutron scattering amplitude at an intermediate wave number adding a small amount of NaBPh_4 in a near-critical D_2O and 3-methylpyridine (3MP) mixture. Such a peak indicates mesophase formation. In the phase diagram of D_2O -3MP, the closed-loop two-phase region shrinks with NaBPh_4 , while it expands with a hydrophilic salt such NaCl [11]. Moreover, they observed multi-lamellar (onion) structures at small volume fractions of 3MP far from the criticality [12, 13]. Afterwards, Leys *et al.* [14] examined the dynamics in D_2O -3MP with NaBPh_4 using dynamic light scattering and small-angle neutron scattering.

We also point out that hydrophilic (hydrophobic) ions can be selectively adsorbed into a water-rich (oil-rich) adsorption layer on a solid wall. This effect is intensified for antagonistic salts, since the disfavored ions are expelled from the layer due to the solvation interaction. Its thickness is microscopic far from the criticality but is widened in its vicinity. The adsorbed ion amount can exceed the bare surface charge of the wall in opposite sign. This is a chemical mechanism of charge inversion [15–17], originating from the selective solvation.

Another interesting effect with antagonistic salts is that the disturbances around solid surfaces become oscillatory in space near the transition to mesophases [18, 19]. This gives rise to oscillatory dependence of the force between two colloidal particles or two parallel walls on their separation distance d . Furthermore, dynamics such as phase ordering and rheology is of great interest. Thus, more experiments are very informative.

In Sec.2, we will present the background of physics and chemistry in aqueous mixtures with antagonistic ion pairs. In Sec.3, we will treat salt-induced mesophases.

*Corresponding author.

Email address: onuki@scphys.kyoto-u.ac.jp (A. Onuki)

II. THEORETICAL BACKGROUND

2.1. Solvation chemical potential

For each solute particle, the solvation part of the chemical potential is written as $\mu_s^i(\phi)$. In mixture solvents, it depends on the water composition ϕ . Let us suppose two species of monovalent ions ($Z_1 = 1$, $Z_2 = -1$). At sufficiently low ion densities, the total ion chemical potential μ_i in a mixture solvent is expressed as

$$\mu_i = k_B T \ln(n_i \lambda_i^3) + Z_i e \Phi + \mu_s^i(\phi), \quad (1)$$

where λ_i is the thermal de Broglie length and Φ is the electric potential. In equilibrium μ_i is homogeneous. The ϕ dependence of $\mu_s^i(\phi)$ has not been well investigated.

We consider a liquid-liquid interface between a water-rich phase α and an oil-rich phase β with bulk compositions ϕ_α and ϕ_β and with bulk ion densities $n_{i\alpha}$ and $n_{i\beta}$. For each ion species i we introduce the difference,

$$\Delta\mu_s^i = \mu_s^i(\phi_\alpha) - \mu_s^i(\phi_\beta), \quad (2)$$

which is the Gibbs energy of transfer in electrochemistry (usually measured in units of kJ/mol)[20–23]. It is negative (positive) for hydrophilic (hydrophobic) ions. The electric potential Φ tends to constants Φ_α in α and Φ_β in β , yielding a Galvani potential difference,

$$\Delta\Phi = \Phi_\alpha - \Phi_\beta = (\Delta\mu_s^2 - \Delta\mu_s^1)/2e, \quad (3)$$

From the charge neutrality in the bulk, we have

$$n_{i\beta}/n_{i\alpha} = \exp[-(\Delta\mu_s^1 + \Delta\mu_s^2)/2k_B T]. \quad (4)$$

For water-nitrobenzene (NB) at $T = 300$ K in strong segregation [2, 20–22], $\Delta\mu_s^i/k_B T$ was -13.6 for Na^+ , -27.1 for Ca^{2+} , and -11.3 for Br^- , while it was 14.4 for BPh_4^- . In the NB-rich phase in this case, the water content is $\phi \sim 0.003$ and well-defined hydration shells are already formed around metallic ions[22]. For water-alcohol [23], $\Delta\mu_s^i$ was observed to be relatively small in weak segregation. For hydrophobic particles, $\mu_s^i(\phi)$ depends on how they deform the surrounding hydrogen bonding, so it increases sharply with increasing their size[3].

2.2. Ginzburg-Landau theory

In our previous papers [4, 6–8], we used the Ginzburg-Landau theory [24] to examine the interface profiles and the phase behavior, where ϕ and n_i are coarse-grained variables. The free energy density is the sum of the electrostatic energy $\varepsilon(\phi)|\mathbf{E}|^2/8\pi$ and f_{tot} given by

$$\begin{aligned} \frac{f_{\text{tot}}}{k_B T} = & \frac{1}{v_0} [\phi \ln \phi + (1 - \phi) \ln(1 - \phi) + \chi \phi(1 - \phi)] \\ & + \frac{1}{2} C |\nabla \phi|^2 + \sum_i n_i [\ln(n_i \lambda_i^3) - 1 - g_i \phi], \end{aligned} \quad (5)$$

where $v_0 = a^3$ is the molecular volume with $a \sim 3$ Å, $\chi(T)$ is the interaction parameter depending on T , and we set $C = a^{-1}$. Though very crude, we use the linear

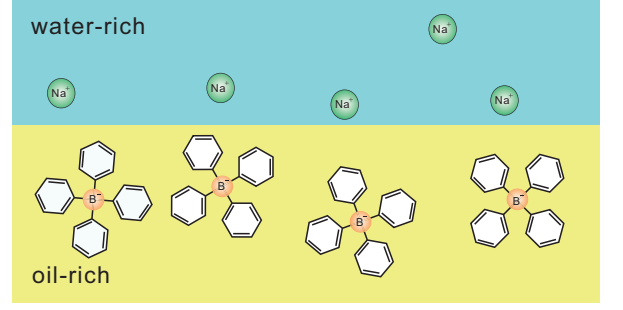


FIG. 1: Hydrophilic Na^+ in water-rich region and hydrophobic BPh_4^- in oil-rich region around an interface.

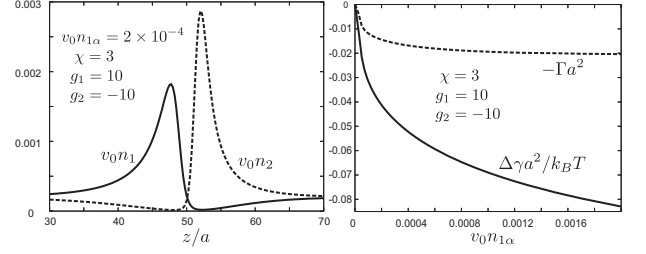


FIG. 2: Left: Interfacial ion densities $n_1(z)$ and $n_2(z)$ multiplied by $v_0 = a^3$ vs z/a for antagonistic pair, where $v_0 n_{1\alpha} = 4 \times 10^{-4}$. Right: Surface tension decrease $\Delta\gamma = \gamma - \gamma_0$ divided by $k_B T / a^2$ and surface ion adsorption Γ multiplied by $-a^2$ vs $v_0 n_{1\alpha}$. Here, $\chi = 3$ and $g_1 = -g_2 = 10$.

form $\mu_s^i(\phi) = A_i - k_B T g_i \phi$, where A_i is a constant. Then, $\Delta\mu_s^i = -k_B T g_i (\phi_\alpha - \phi_\beta)$. In our theory, g_i represents the solvation strength. The electric field $\mathbf{E} = -\nabla \Phi$ satisfies the Poisson equation $\nabla \cdot \varepsilon \mathbf{E} / 4\pi = \rho = e(n_1 - n_2)$, where the dielectric constant depends on ϕ as $\varepsilon(\phi) = \varepsilon_0 + \varepsilon_1 \phi$. In this work, we set $\varepsilon_1 = \varepsilon_0$ and $e^2 / \varepsilon_0 k_B T = 3a$.

For large $|g_i| \gg 1$, the phase behavior from our model is complicated even for small n_i . See the mean-field phase diagram in our previous paper[8]. Let a homogeneous solution have mean water concentration ϕ and mean ion densities $n_1 = n_2 = n_e$. A linear instability occurs for

$$\tau < (g_1 + g_2)^2 n_e / 2 + 8\pi \ell_B C (\gamma_p - 1)^2 n_e. \quad (6)$$

Here, $\tau = [1/\phi(1 - \phi) - 2\chi]/v_0$ is the second derivative of the first term in Eq.(5) with respect to ϕ , $\ell_B = e^2 / \varepsilon k_B T$ is the Bjerrum length, and the parameter

$$\gamma_p = (16\pi C \ell_B)^{-1/2} |g_1 - g_2| \quad (7)$$

represents the strength of antagonicity. The Debye wave number is $\kappa = (8\pi \ell_B n_e)^{1/2}$. If Eq.(6) holds with $\gamma_p > 1$, the fluctuations with wave number $q_m = \kappa(\gamma_p - 1)^{1/2}$ grow to form a periodic structure.

2.3. Interface profiles

In Fig.2, we display typical ion profiles near an interface (left) along the z axis, where hydrophilic cations and hydrophobic anions are separated on the scale of the

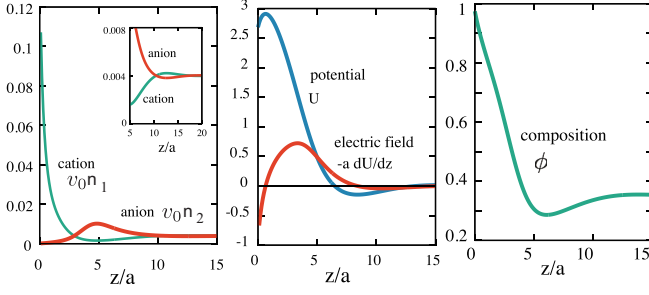


FIG. 3: Profiles near hydrophilic wall with surface charge density $\sigma_0 = -0.04ea^{-2}$ at $z = 0$, where $\chi = 2$, $g_1 = -g_2 = 10$, and $v_0 n_i \rightarrow 4 \times 10^{-3}$ as $z \rightarrow \infty$. (a) Ion densities, where cations are adsorbed near the wall in excess of $\sigma_0 < 0$. They are expanded in region $5 < z/a < 20$ (inset). (b) Normalized potential $U = e\Phi/k_B T$ and electric field $-a dU/dz = (ea/k_B T)E$. (c) Composition ϕ , tending to 0.35 as $z \rightarrow \infty$.

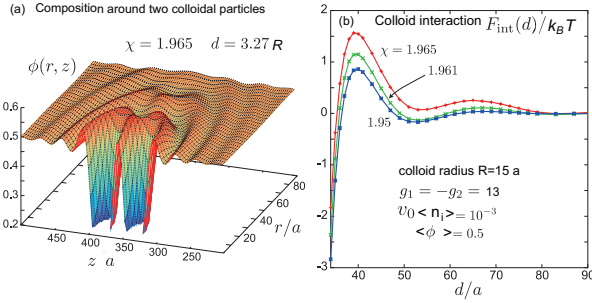


FIG. 4: Two hydrophobic colloidal particles with radius $R = 15a$ and separation $d = 3.27R$ without surface charges [18], where $\chi = 1.965$, $g_1 = -g_2 = 13$, $v_0 \langle n_i \rangle = 10^{-3}$, and $\langle \phi \rangle = 0.5$. (a) Composition $\phi(r, z)$ in the r - z plane, where $r = (x^2 + y^2)^{1/2}$. (b) Normalized interaction free energy $F_{\text{int}}(d)/k_B T$ vs d/a for $\chi = 1.950, 1.961$, and 1.965 .

Debye length $\kappa^{-1} (\sim 10a)$. In the right panel, we show the surface tension deviation $\Delta\gamma = \gamma - \gamma_0$ and the ion adsorption Γ vs the ion density $n_{1\alpha}$ in phase α . Here, γ_0 is the surface tension without ions and Γ is the integral of $n(z) - n_\alpha - (\phi(z) - \phi_\alpha)(n_\beta - n_\alpha)/(\phi_\beta - \phi_\alpha)$ with $n = n_1 + n_2$. For small ion densities, γ is given by [4, 6]

$$\gamma \cong \gamma_0 - k_B T \Gamma - \int dz \varepsilon |\mathbf{E}|^2 / 8\pi. \quad (8)$$

The third electrostatic term is of order $-\kappa\varepsilon_0|\Delta\Phi|^2/4\pi$ in terms $\Delta\Phi$ in Eq.(3), dominating over the second Gibbs term. We may realize $\gamma < 0$ with increasing the salt amount and/or approaching the solvent criticality.

2.4. Selective ion adsorption on a wall

In Fig.3, we plot profiles near a hydrophilic wall, where we impose the boundary condition $d\phi/dz = -0.2/a$ at $z = 0$. Here, the cations are accumulated in the adsorption layer ($z/a \lesssim 4$), while the anions are expelled from it. For simplicity, we neglect the image interaction. The

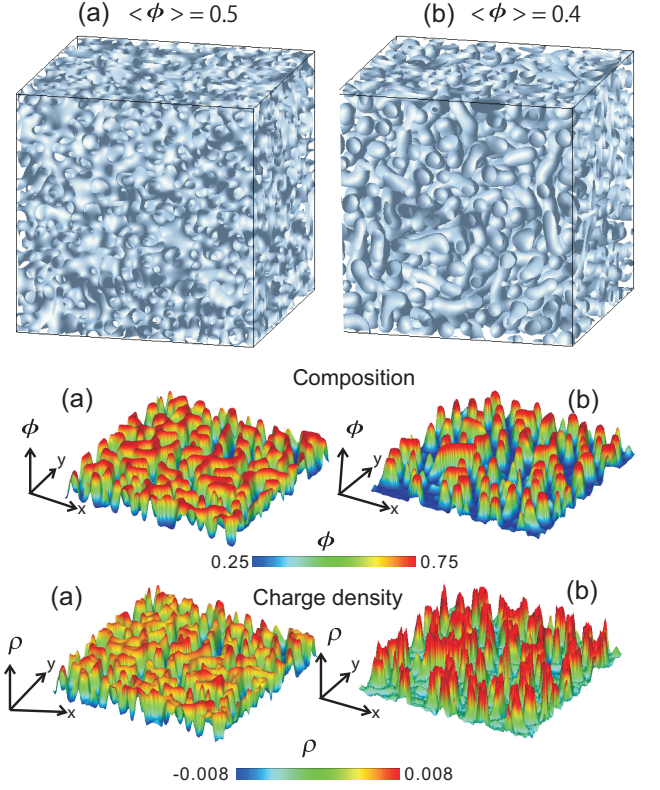


FIG. 5: Mesophase patterns near solvent criticality induced by antagonistic salt. They are calculated in a box of length $128a$ with $\chi = 2$, $g_1 = -g_2 = 10$, and $v_0 \langle n_i \rangle = 7.3 \times 10^{-4}$. Average composition $\langle \phi \rangle$ is (a) 0.5 (left) and (b) 0.4 (right). These patterns are nearly stationary without thermal noises. Top: Surfaces of $\phi(\mathbf{r}) = 0.5$, which are (a) bicontinuous and (b) tubelike. Middle: Cross-sectional profiles of composition $\phi(x, y, 0)$. Bottom: Those of charge density $\rho(x, y, 0)$. The colors represent $e\Phi/k_B T$ according to the color bar.

electric field E along the z axis is given by

$$\varepsilon(z)E(z)/4\pi = \sigma_0 + \int_0^z dz' \rho(z'). \quad (9)$$

The surface charge density is $\sigma_0 = -0.04ea^{-2}$. As a result, we find $E < 0$ for $z/a < 0.7$ and $E > 0$ in an intermediate range $0.7 < z/a < 8.4$. For larger z , E is very small and is oscillating.

Thus, both adsorption and desorption of ions take place simultaneously on solid surfaces with antagonistic salts in mixture solvents. However, highly hydrophobic ions such as AsPh_4^+ (tetraphenylarsenate) [16] and BPh_4^- [17] are absorbed on hydrophobic colloid surfaces in water (without oil) leading to charge inversion.

2.5. Spatially oscillating disturbances

Let us assume that τ is slightly larger than the right hand side with $\gamma_p > 1$ in Eq.(6) [18, 19]. In this case, the deviations of the composition and the electric potential are strongly coupled. As a result, oscillatory disturbances

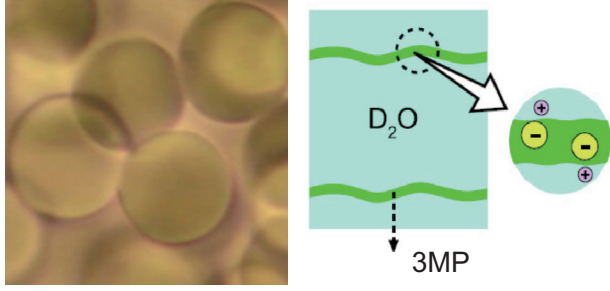


FIG. 6: Left: Optical microscopic image of onions with radius about 10^4 nm at $T = 313$ K in D_2O -3MP with $NaBPh_4$ (0.085 mol/L) far from criticality, where D_2O volume fraction is 0.91 (taken from Ref.[12]). Right: Illustration of lamellar structure, where spacing is 17.5 nm and membranes consisting of 3MP and BPh_4^- have thickness about 1.6 nm.

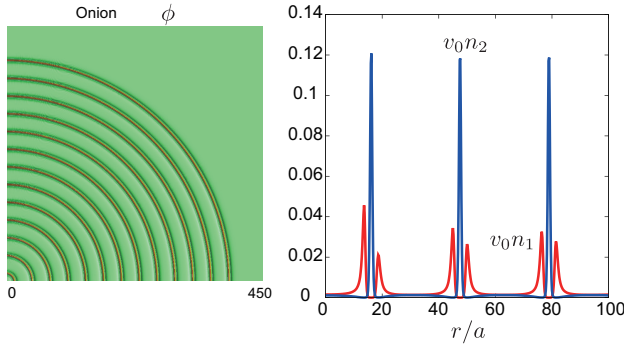


FIG. 7: Numerically calculated onion, where $\chi = 2.25$, $g_1 = -g_2 = 15$, $\langle \phi \rangle = 0.8$, and $v_0 \langle n_i \rangle = 3 \times 10^{-3}$. Membranes are composed of oil and hydrophobic anions. (a) Cross-sectional profile of composition $\phi(r)$ (r is the distance from the center). (b) Those of $v_0 n_1(r)$ and $v_0 n_2(r)$ around 3 membranes.

appear around colloidal particles [18] or between parallel solid walls [19] in equilibrium.

In Fig.4, we show a wavelike profile $\phi(r, z)$ around two colloidal particles with radius $R = 15a$ at $\chi = 1.965$ [18], where $r = (x^2 + y^2)^{1/2}$. The center-to-center distance is $d = 3.27R$. Their surfaces are surrounded by oil layers rich in hydrophobic anions without surface charges. They are effectively charged as in Fig.3. No van der Waals interaction is assumed. In the right panel, the interaction free energy $F_{\text{int}}(d)$ of the two particles is plotted as a function of d . Instability to a mesophase occurs for $\chi > 1.9651$, so homogeneity is attained far from the particles. Here, $F_{\text{int}}(d)$ exhibits a shallow minimum at $d \sim 80a$ and a maximum of order $k_B T$ at $d \sim 40a$. The maximum increases as R^2 with increasing the radius R , so it can prevent contact of the particles for large R .

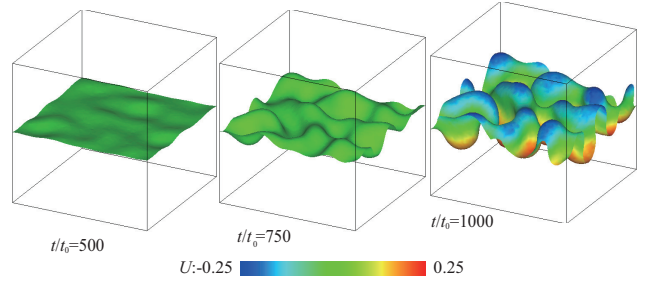


FIG. 8: Growth of interface deformations induced by antagonistic salt [25] in a box of length $64a$ at $t/t_0 = 500, 750$, and 1000 , where $t_0 = 2\pi a^3 \eta / k_B T$. The ion diffusion constant is $D = a^2/t_0$ for the two species. Here, $\chi = 2.1$ and $g_1 = -g_2 = 12$. The colors represent $U = e\Phi/k_B T$.

III. MESOPHASE FORMATION

3.1. Mesophases near criticality

To calculate mesophase structures near the criticality[10, 11], we changed χ from a small value to $\chi_c = 2$ at $t = 0$, where Eq.(6) is satisfied with $\gamma_p = 1.4$. We used model H equations with viscosity η [7, 8, 24]. The random patterns in Fig.5 are those at $t = 1000t_0$ with $t_0 = 2\pi a^3 \eta / k_B T$, which are nearly stationary without thermal noises in the dynamic equations. The domain sizes are on the order of the Debye length κ^{-1} . For (a) $\langle \phi \rangle = 0.5$, we can see bicontinuous patterns, resembling those in spinodal decomposition at a critical quench [24]. For (b) $\langle \phi \rangle = 0.4$, tubelike domains appear, where the droplet volume fraction (of the region $\phi > 1/2$) is 0.25. Remarkably, the droplets are considerably elongated. The degree of elongation increases with increasing the salt amount (not shown in this paper). In the lower panels, we give the cross-sectional profiles of ϕ and $\rho = e(n_1 - n_2)$. We can see that the domains with $\phi > \langle \phi \rangle$ ($\phi < \langle \phi \rangle$) are positively (negatively) charged.

With further increasing χ inside the two phase region, a changeover should occur from random mesophases into macroscopic two-phase states. In real near-critical systems, these mesophase fluctuations are thermally changing in time and their influence on the static and dynamic critical behaviors remains unclear [11, 14].

3.2. Onions

Second, as illustrated in Fig.6, Sadakane *et al.* [12, 13] observed onions of many membranes (~ 500) composed of 3MP and BPh_4^- . The lamellar spacing is 17.5 nm and the membrane thickness is 1.6 nm. These onions are due to strong hydrophobicity of BPh_4^- in a water-rich environment. The membranes are analogous to those of ionic surfactants and the adsorbed BPh_4^- density on them is of order 0.01 \AA^{-2} .

We have also performed simulation to find a similar onion in Fig.7, where $\chi = 2.25$, $g_1 = -g_2 = 15$, and $\langle \phi \rangle = 0.8$. We have minimized the free energy in the spherically symmetric geometry in the region $0 < r < 500a$, where r

is the distance from the center. The lamellar spacing and thickness are $32a$ and $6a$, respectively. The adsorption of the anions within each membrane is $0.116a^{-2}$ per unit area. The composition $\phi(r)$ is 0.827 outside the membranes (commonly within and outside the onion), while the average composition within the membranes becomes about 0.5.

3.3. Interface instability

In Fig.8, we also numerically examine the interface instability [25] with $\chi = 2.1$ and $g_1 = -g_2 = 12$ in a cubic cell with length $L = 64a$. At $t = 0$, an interface was at $z = L/2$ and we added antagonistic ion pairs to the water side, where $\langle n_i \rangle = 0.006v_0^{-1}$ for $z > L/2$ and $\langle n_i \rangle = 0$ for $z < L/2$. We used the model H equations and the ion diffusion equations. Here, surface disturbances grow after appearance of an electric double layer in Fig.2.

We also predict droplet instability induced by an antagonistic salt. It is of interest how planar or spherical interfaces are deformed and proliferated into lamellae in the late stage of the instability.

IV. SUMMARY AND REMARKS

We have briefly reviewed the recent research on antagonistic salts in water-oil solvents. Note that the selective

solvation has not been accounted for in the previous electrolyte theories, though it yields a variety of unexplored effects [2]. Antagonistic salts should be one of the most unique entities in these problems, though we have not yet well understood the puzzling observations by Sadakane *et. al* [10–13]. In particular, it is of interest how addition of an antagonistic salt changes the nature of the solvent criticality [8, 11, 14], where the periodic fluctuations appear for $\gamma_p > 1$ as in Fig.5. .

A new aspect highlighted in this work is that antagonistic salts undergo microphase separation near solid surfaces in mixture solvents, as well as across water-oil interfaces. Intriguing is then the behavior of antagonistic salts around proteins or Janus particles having hydrophilic and hydrophobic surface parts.

Acknowledgments

This work was supported by KAKENHI (No. 25610122) and Grants-in-Aid for Japan Society for Promotion of Science (JSPS) Fellows (Grants No. 241799 and 263111).

-
- [1] Israelachvili JN. Intermolecular and surface forces. 2nd ed. London: Academic Press; 1992.
 - [2] Onuki A, Okamoto R, Araki T. Phase transitions in soft matter induced by selective solvation. Bull Chem Soc Jpn 2011; 84, 569-87.
 - [3] Chandler D. Interfaces and the driving force of hydrophobic assembly, Nature 2005; 437: 640-7.
 - [4] Onuki A. Ginzburg-Landau theory of solvation in polar fluids: Ion distribution around an interface. Phys Rev E 2006; 73: 021506 (16 pages).
 - [5] Luo G, Malkova S, Yoon J, Schultz DG, Lin B, Meron M, Benjamin I, Vanysek P, Schlossman ML. Ion distributions near a liquid-liquid interface. Science 2006; 311: 216-8. .
 - [6] Onuki A. Surface tension of electrolytes: Hydrophilic and hydrophobic ions near an interface. J Chem Phys 2008; 128 : 224704 (9 pages).
 - [7] Araki T, Onuki A. Dynamics of binary mixtures with ions: dynamic structure factor and mesophase formation. J Phys: Condens Matter 2009; 21 : 424116-24.
 - [8] Onuki A, Araki T, Okamoto R. Solvation effects in phase transitions in soft matter. J Phys: Condens Matter 2011; 23 : 284113-25.
 - [9] Michler M, Shahidzadeh N, Westbroek M, van Roij R, Bonn D. Langmuir 2015;31:906-11.
 - [10] Sadakane K, Seto H, Endo H, Shibayama M. A periodic structure in a mixture of D₂O-3-methylpyridine/NaBPh₄ induced by solvation effect. J Phys Soc Jpn 2007; 76 : 113602-4.
 - [11] Sadakane K, Iguchi Nagao NM, Endo H, Melnichenko YB, Seto H. 2D-Ising-like critical behavior in mixtures of water and 3-methylpyridine including antagonistic salt or ionic surfactant. Soft Matter 2011; 7: 1334-40.
 - [12] Sadakane K, Onuki A, Nishida K, Koizumi S, Seto H. Multilamellar structures induced by hydrophilic and hydrophobic ions added to a binary mixture of D₂O and 3-methylpyridine. Phys Rev Lett 2009; 103: 167803 (4 pages).
 - [13] K. Sadakane K, Nagao M, Endo H, Seto H. Membrane formation by preferential solvation of ions in mixture of water, 3-methylpyridine, and sodium tetraphenylborate. J Chem Phys 2013; 139: 234905-15.
 - [14] Leys J, Subramanian D, Rodezno E, Hammouda B, Anisimov MA. Mesoscale phenomena in solutions of 3-methylpyridine, heavy water, and an antagonistic salt. Soft Matter 2013; 9: 9326-35.
 - [15] Lyklema J. Overcharging, charge reversal: Chemistry or physics ?, Colloids Surf. A 2006; 291: 3-12.
 - [16] Martin-Molina A, Calero C, Faraudo J, Quesada-Páez M, Travesset A, Hidalgo-Álvarez R. The hydrophobic effect as a driving force for charge inversion in colloids. Soft Matter 2009; 5: 1350-3
 - [17] Calero C, Faraudo J, Bastos-González D. Interaction of Monovalent Ions with Hydrophobic and Hydrophilic Colloids: Charge Inversion and Ionic Specificity. J. Am. Chem. Soc. 2011; 133: 15025-35.
 - [18] Okamoto R, Onuki A. Charged colloids in an aqueous mixture with a salt. Phys Rev E 2011; 84: 051401-19.
 - [19] Pousaneh F, Ciach A. The effect of antagonistic salt on a confined near-critical mixture. Soft Matter 2014; 10: 8188-201.

- [20] Hung LQ. Electrochemical properties of the interface between two immiscible electrolyte solutions. *J Electroanal Chem* 1980; 115: 159-74.
- [21] Koryta J. Electrochemical polarization phenomena at the interface of two immiscible electrolyte solutions-II. *Electrochim. Acta* 1984; 29: 445-52.
- [22] Osakai T, Ebina K. Non-Bornian theory of the Gibbs energy of ion transfer between two immiscible liquids. *J Phys Chem B* 1988; 102: 5691-8.
- [23] Kalidas C, Hefter G, Marcus Y. Gibbs energies of transfer of cations from water to mixed aqueous organic solvent. *Chemical Rev* 2000; 100: 819-52.
- [24] Onuki A. Phase transition Dynamics. Cambridge: Cambridge university press: 2002.
- [25] Onuki A, Araki T. Selective Solvation in aqueous mixtures: interface deformations and instability. *J Phys Soc Jpn* 2012; 81: SA004-12.